PROCEEDINGS OF SCIENCE

ONLINE ICRC 2021
THE ASTROPARTICLE PHYSICS CONFERENCE
Berlin | Germany
37th International Cosmic Ray Conference
12–23 July 2021

Reconstruction of Nearly Horizontal Muons in the HAWC Observatory

Ahron S. Barber[a], David B. Kieda[a], and R. Wayne Springer*[a] on behalf of the HAWC Collaboration

(a complete list of authors can be found at the end of the proceedings)

aDepartment of Physics and Astronomy, University of Utah, Salt Lake City, UT, USA

E-mail: wayne.springer@utah.edu

The volcanoes surrounding the HAWC observatory provide varying material depths from open sky to over 15 km of rock for nearly horizontal muon trajectories. The muon integral intensity as a function of material depth may be determined from the rate of muons as a function of arrival direction near the horizon. A Hough transform algorithm is used to identify nearly-horizontal muons traversing the HAWC observatory by finding a line in the 3d point cloud of PMT hits (x_i,y_i, and ct_i). The arrival direction of the muon can be estimated from this line. Background Extensive Air Shower (EAS) fragments are identified by the presence of a lateral extension of PMT hits in a plane normal to the muon candidate trajectory. A geometry-based simulation has been developed to improve and estimate arrival direction reconstruction resolution and effective area. A description of the reconstruction techniques and estimates of detector resolution, backgrounds, and effective area as a function of arrival direction, will be provided.

37th International Cosmic Ray Conference
12-23 July 2021
Berlin Germany/Online

*Speaker

PoS(ICRC2021)254

1. INTRODUCTION

The High Altitude Water Cherenkov Observatory, HAWC, is designed to detect VHE Gamma-Ray and Cosmic-Ray extensive air shower (EAS) events. HAWC consists of 300 Water Cherenkov Detectors (WCD) arranged in an array covering approximately 22,000 m^2 at an altitude of 4100 m at the saddle point between two volcanoes, Sierra Negra and Pico de Orizaba in Mexico. Each WCD contains about 200,000 L of water in a cylindrical bladder 7.3 m in diameter and 4.3 m in height. Four upward-looking PMTs view the water volume from the floor of each WCD. The absolute location of each PMT is surveyed to a precision of approximately 1cm in each direction. The surface over which the tanks are deployed is flat but at an angle of roughly 0.7 degrees from the horizontal path just slightly west of north. The PMTs measure the arrival time of Cherenkov light generated by relativistic charged particles to a precision of better than 1 ns. As shown in figure 1, the regular arrangement of the WCDs and PMTs facilitates the operation of the HAWC observatory as a hodoscope that can detect and measure the trajectory of nearly horizontal muons, as described in [1]. In addition, the surrounding volcanoes provide material depths up to 30 km water equivalent (km w.e.) for a considerable fraction of the acceptance of HAWC, thereby enabling a measurement of the intensity of muons as a function of depth. This effort was motivated to perform studies of cosmic ray composition by studying muon multiplicity and rates as described in [2].

Figure 1 The HAWC observatory and Pico de Orizaba. Three hundred WCDs arranged in a regular array can be utilized as a hodoscope to observe nearly horizontal muons.

Previous measurements of muon intensity as a function of depth from underground observatories have been compiled by Bugaev[3]. A notable feature of the spectra is its flattening for depths above 14,000 hg cm^{-3} (or 14 km w.e) due to the constant intensity of neutrino-induced muons. Preliminary results from HAWC, as reported in the ICRC 2019 proceedings paper on a measurement of the integral intensity of nearly horizontal muons[4], are consistent with the muon intensity as a function of depth with significant uncertainties up to depths of 7 km. However, background events from misidentified EAS events, muons scattered from the mountain surface into the acceptance of HAWC [5], and poorly reconstructed muon events from directions of less depth have dominated the signal for muons penetrating depths over 6 km. We are attempting to improve the reconstruction of the trajectories of nearly horizontal muons as described in this report to reduce the background from poorly reconstructed muon trajectories. We are also incorporating the improved reconstruction algorithms into acceptance calculations as described below.

2. MUON TRAJECTORY RECONSTRUCTION

To fully reconstruct the trajectory of the muon, both the arrival direction (azimuth and zenith angles) and offset from the center of the plane normal to the arrival direction must be determined. It is crucial to reasonably measure the offset for arrival directions where the depth is rapidly changing, such as the edges of the volcanoes. For each of the three arrival directions shown in figure 2, one of the two shown trajectories is intercepted by the volcano depending upon its offset in either the lateral or vertical direction. It is possible to "mask" the regions where the depth is rapidly changing and exclude those regions from analysis as described in [4]. We utilize a modified version of the three-dimensional Hough transformation software developed by the Dalitz group [6]. This software identifies data consistent with straight lines in a 3d point cloud with user-configured resolution. Our implementation of this software to identify muons and reject EAS background was described by [4] in detail.

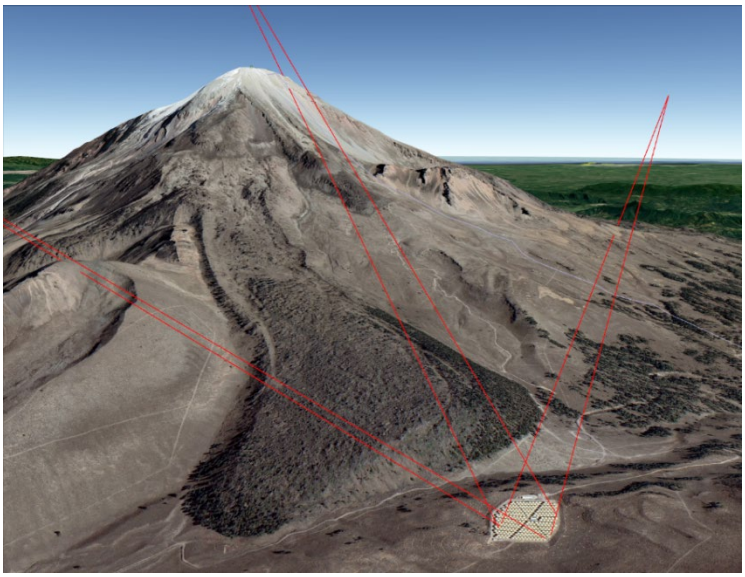

Figure 2 Muon trajectories (red lines) with differing offsets for three arrival directions.

We have expanded the previous reconstruction procedure using the Hough transform by implementing a least-squares minimization to determine trajectory parameters (azimuth and zenith angles and the lateral and vertical offsets) and their uncertainties. The uncertainties are obtained from the slope parameters determined by linear least-squares techniques and propagation of errors described in Taylor's standard undergraduate laboratory text [7]. This simple method can be performed for both simulated and actual data for individual events directly from the PMT hit information. The point cloud of PMT hits as indicated by the 2d spatial coordinates, and the hit time multiplied by the speed of light is shown in the upper portion of figure 3. The 3d Hough algorithm identifies the points associated with linear nearly horizontal propagation consistent with the speed of light. The "Hough line" is projected onto the HAWC observatory plane to determine the azimuthal arrival direction ϕ. An apparent propagation speed v_{app} for the muon is determined from the slope of the fitted "Hough line" to the data points ct_i vs $\sqrt{x_i^2 + y_i^2}$. The zenith angle θ is determined from the difference of v_{app}, with the speed of light in vacuum c, using the equation $\theta = 90^0 - \sin^{-1}((v_{app} / c) - 1)$.

An assessment of the expected uncertainties for a complete sampling of the phase space will be used to determine the acceptance and arrival direction resolution for each arrival direction and offset. The acceptance as a function of depth can be determined by correlating the depth vs. arrival direction from GIS data [8].

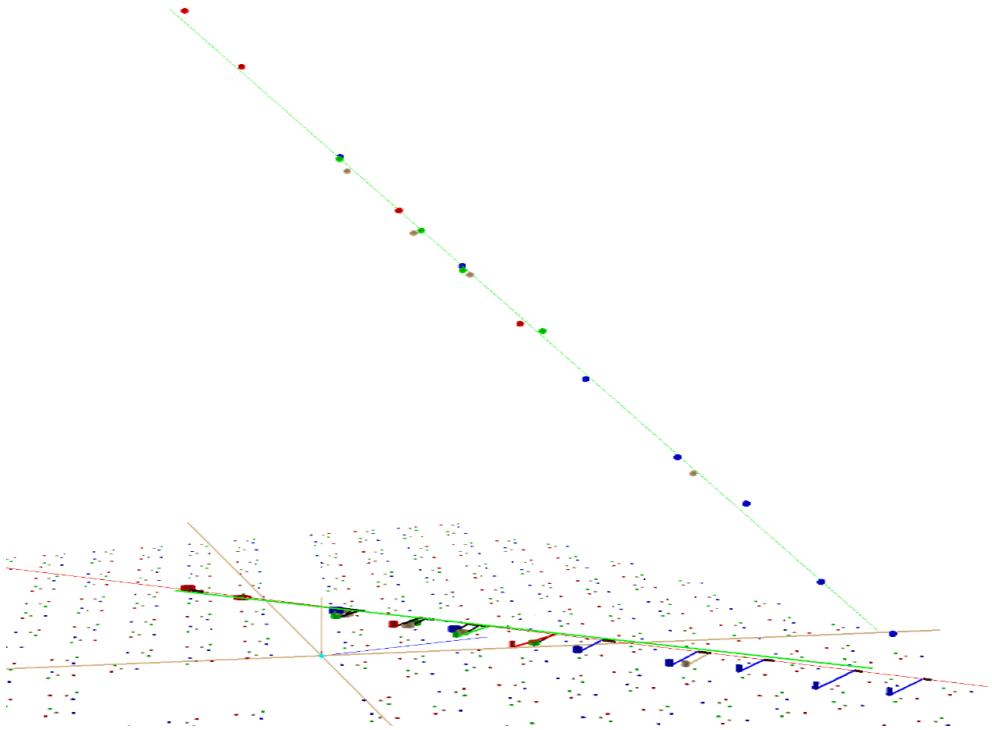

Figure 3 A simulated muon trajectory (red line) and the calculated PMT hits and reconstructed muon trajectory (thicker green line). The array of PMTs are indicated by colored markers in the detector plane. The point cloud of the coordinates of PMT hits, x_i, y_i, ct_i , are shown by the colored dots above the plane in each panel. The 3d Hough algorithm identifies the PMT hits associated with linear, nearly horizontal, propagation consistent with the speed of light. The 3d Hough line (thin green) is projected onto the HAWC observatory plane to determine the azimuthal arrival direction. The difference of the apparent speed from the speed of light in vacuum is used to determine the zenith angle indicated in the thick green line just above the detector plane.

3. SEMI-ANALYTIC SIMULATION OF PMT RESPONSE TO MUONS

A semi-analytic geometry-based technique to simulate the response of HAWC to the passage of nearly horizontal muons has been developed to assess the resolution of the muon trajectory measurements and the detector acceptance as a function of arrival direction and offset. The WCD tanks intersected by a given muon trajectory are found by determining the minimum distance from tank centers to the trajectory line. WCD tanks whose centers have a projected horizontal distance less than a tank radius are considered "hit," and their PMT response to a simplified Cherenkov emission from the muon trajectory is determined. It is determined for each PMT in a "hit" tank whether direct (un-reflected) Cherenkov emission can be seen by finding the line whose angle is at the Cherenkov emission angle intersects the center of the PMT. If such a line exists

and the intersection point with the muon trajectory lies inside the tank, the PMT is considered a "hit." The time at which the muon first enters the tank since the start of its journey is calculated. The time that the PMT is hit after the tank entry time of the muon is calculated by determining the muon travel time, assuming $v_{muon} = c$, to the Cherenkov emission point and adding the propagation time of the Cherenkov light $v_{Cherenkov} = c / n_{H_2O}$ to the PMT center. The PMT hit time is then the sum of these times. The charge of the PMT is estimated by the fraction of the circumference of the Cherenkov ring subtended by a hemisphere of the diameter of the PMT (either 8" or 10") at the location of the PMT. The number of photons emitted in a Cherenkov ring is a parameter that has been adjusted to give a mean number of observed photoelectrons to be about 10, as seen in the data. A Gaussian with adjustable width, typically 1ns (0.4 ns determined from calibration), randomizes the PMT time. The number of photoelectrons is randomized using Poisson fluctuation of the expected number from the calculation. Figure 4 shows the simulated response of PMTs to a given muon trajectory (red line). The diameters of the colored rings indicate charge. The vertical position of the colored spheres indicates the PMT time (multiplied by the speed of light). This simulation will estimate the arrival direction and offset measurement resolution as a function of the arrival direction. The estimated resolution will be used as a basis to determine if that trajectory contributes to the detector acceptance, as described in the next section.

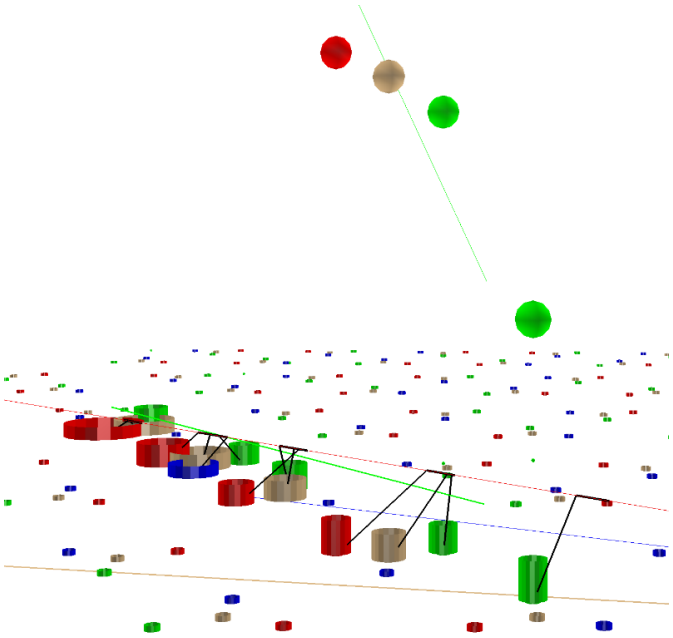

Figure 4 Simulated PMT response to a muon. The lines from the PMT centers to the muon trajectory indicate the Cherenkov path from its emission point from the muon trajectory. The reconstruction procedure itself determines the uncertainty in the measurement of azimuth and zenith angles as well as offsets on an event-by-event basis. The bias of the reconstruction may also be measured from the simulated events as shown by the difference in the thrown (red) and reconstructed (green) trajectories.

4. ESTIMATION OF RESOLUTION

We use the semi-analytic simulation to determine the bias and estimated uncertainty in reconstruction as a function of arrival direction and offset. The determination of trajectory resolution is performed by comparing the simulated response of the detector PMT hits to muon trajectories varied about a nominal trajectory. A chi-square statistic, $\chi^2 = \sum_{i=1}^{N} \frac{\left(y_i - f\left(x_i\right)\right)^2}{\sigma_i^2}$, is formed for both timing and charge information. The semi-analytic simulation plays the role of

the "fit-function" $f(x_i)$ while y_i is either the PMT charge or time. The charge is measured in units of photoelectrons, $y_i = npe_{ihit}$ whose uncertainty is $\sigma_i = \sqrt{npe_{ihit}}$. The uncertainty in time $y_i = t_{ihit}$ is given by the measured PMT timing resolution. A variation of the reduced chi-square by a factor of 1 may estimate the resolution in a measurement parameter. For a simulated trajectory that can be well reconstructed, the reduced chi-square of the PMT times as a function of azimuth and zenith angle is shown in Figures 5, 6, and 7 for a representative trajectory that can be well reconstructed. This technique shows that the comparison of timing information for different muon trajectories allows a determination of both zenith and azimuth to better than 0.5 degrees for, particularly preferred directions.

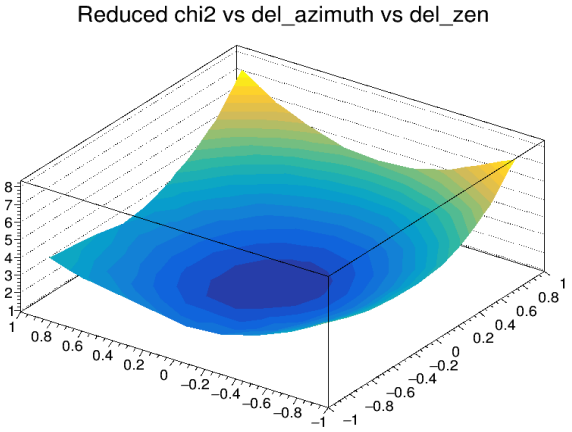

Figure 5 Reduced chi-square from timing information vs Δ_ϕ vs Δ_θ for a simulated representative trajectory that can be well reconstructed. The differences in the the trial azimuth and zenith direction direction about nominal trajectory are given by $\Delta_\phi = \phi_{\text{nominal}} - \phi_{\text{trial}}$ and $\Delta_\theta = \theta_{\text{nominal}} - \theta_{\text{trial}}$. The jitter of PMT timing was assumed to be 1.0 ns.

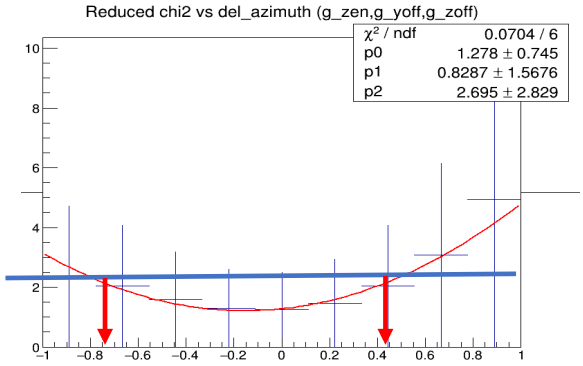

Figure 6 *Estimation of uncertainty* for a simulated trajectory *on azimuth direction obtained from change in chi-square value of 1 indicates that the range in* Δ_ϕ lies between $(-0.7^0, 0.45^0)$ *with a bias of* -0.125^0 *and a resolution of* $\sigma_\phi = 0.57^0$.

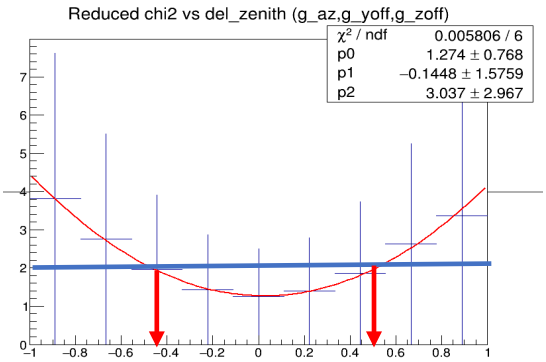

Figure 7 Estimation of uncertainty for a simulated trajectory on zenith direction obtained from change in chi-square value for timing of 1 indicates that the range in Δ_θ *lies between* $(-0.4^0, 0.45^0)$ with a bias of 0.025^0 and a resolution of $\sigma_\theta = 0.47^0$.

5. ESTIMATION OF DETECTOR ACCEPTANCE

The detector acceptance as a function of arrival direction may be estimated using the semi-analytic simulation of the PMT response described in section 3. Trial trajectories covering the available phase space covering zenith, azimuth, lateral offset, and vertical offset $\theta, \phi, y_{off}, z_{off}$ can be examined as shown in figure 8. Those trajectories that can be reconstructed with acceptable uncertainty and bias will contribute an area and solid angle to the total detector acceptance. The acceptance as a function of arrival direction and offset can thereby be determined. Correlating this information with depth as a function of trajectory enables the determination of detector acceptance vs depth.

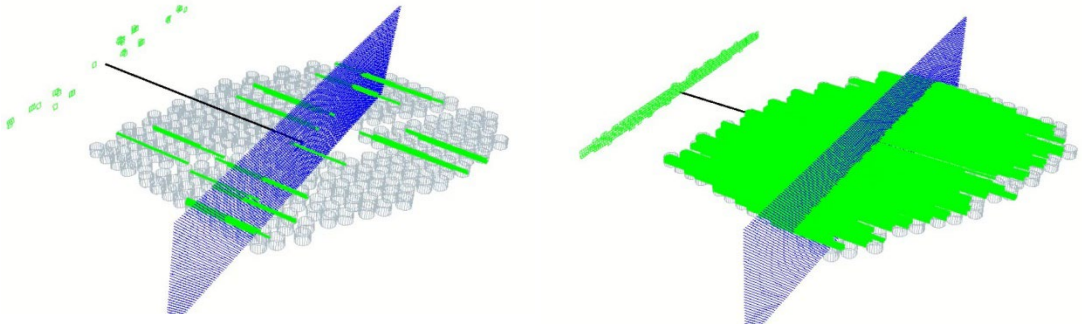

Figure 8 Illustrations showing procedure to estimate acceptance by summing the effective area (green squares to left of panels) associated with many muon trajectories for a given arrival direction(black line). All muon trajectories shown are for an azimuthal direction of 121° . Those with zenith angle of 83.25 ° are shown in the left panel. Those with zenith angle 90.75 ° are shown in the right panel. The green lines indicate the reconstructed track length for muon trajectories. The area associated for that trajectory element of phase space is added to the detector acceptance if the track length exceeds a required minimum. The panel on the right shows that for the preferred direction of $\phi = 121.0^o$,$\theta = 90.75^o$ where the effective detector area approaches the geometric cross-sectional area of HAWC viewed from the detector plane that is inclined in that azimuthal direction by approximately 0.75^o.

6. CONCLUSION

It is planned to measure the observed number of muons satisfying well-modeled selection criteria as a function of arrival direction and offset for the considerable exposure time of many years of HAWC observatory operation. The selection criteria will be chosen to reduce backgrounds from EAS as well as mis-reconstructed trajectories as much as possible. The acceptance determination for the same criteria will be estimated using the semi-analytic simulation described above. A measurement of muon intensity vs. depth will be determined using the HAWC observatory for depths above the limiting depth of 6 km, as reported previously. The detailed simulation studies will estimate the backgrounds and sensitivity to provide limits on the muon intensity at the greatest depths possible, which hopefully exceed 14 km w.e where neutrino induced muons could be observed.

References

[1] Ahron Barber, David Kieda, R. Wayne Springer for the HAWC Collaboration, *Detection of Near Horizontal Muons with the HAWC Observatory*, HAWC Collaboration (Ahron S. Barber *et al.*). Oct 11, 2017. 8 pp. HAWC-ICRC-2017-31, Conference: C17-07-12 Proceedings

[2] Ahron Barber, David Kieda, R. Wayne Springer for the HAWC Collaboration, *Simulation of Near Horizontal Muons and Muon Bundles for the HAWC Observatory with CORSIKA*, HAWC Collaboration (Ahron S. Barber *et al.*). Oct 11, 2017. 8 pp. HAWC-ICRC-2017-31, Conference: C17-07-12 Proceedings

[3] Bugaev, E. V. and Misaki, A. and Naumov, V. A. and Sinegovskaya, T. S. and Sinegovsky, S. I. and Takahashi, N., *Atmospheric muon flux at sea level, underground*, and underwater, doi 10.1103/PhysRevD.58.054001

[4] Ahron Barber, David Kieda, R. Wayne Springer for the HAWC Collaboration, *Measurement of the Integral Intensity of NearHorizontal Muons with HAWC*, Proceedings of Science for the 36th International Cosmic Ray Conference (ICR2019),

[5] H. León Vargas, *Characterization of the background for a neutrino search with the HAWC observatory,* Submitted to PhysRevD.

[6] Christoph Dalitz, Tilman Schramke, and Manuel Jeltsch, Iterative Hough Transform for Line Detection in 3D Point Clouds, Image Processing On Line, 7 (2017), pp. 184–196. https://doi.org/10.5201/ipol.2017.208

[7] Taylor, J.R. (1997) An Introduction to Error Analysis: The Study of Uncertainties in Physical Measurements. 2nd Edition, University Science Books, Sausalito.

[8] Instituto Nacional de Estadística y Geografía (INEGI) Continuo de elevaciones mexicano 3.0 (cem3.0), 2012. https://www.inegi.org.mx/app/geo2/elevacionesmex/

Acknowledgements

We acknowledge the support from: the US National Science Foundation (NSF); the US Department of Energy Office of High-Energy Physics; the Laboratory Directed Research and Development(LDRD) program of Los Alamos National Laboratory; Consejo Nacional de Ciencia y Tecnología(CONACyT), México, grants 271051, 232656, 260378, 179588, 254964, 258865, 243290, 132197,A1-S-46288, A1-S-22784, cátedras 873, 1563, 341, 323, Red HAWC, México; DGAPA-UNAMgrants IG101320, IN111716-3, IN111419, IA102019, IN110621, IN110521; VIEP-BUAP; PIFI2012, 2013, PROFOCIE 2014, 2015; the University of Wisconsin Alumni Research Foundation; theInstitute of Geophysics, Planetary Physics, and Signatures at Los Alamos National Laboratory; Polish Science Centre grant, DEC2017/27/B/ST9/02272; Coordinación de la Investigación Científicade la Universidad Michoacana; Royal Society - Newton Advanced Fellowship 180385; Generalitat Valenciana, grant CIDEGENT/2018/034; Chulalongkorn University's CUniverse (CUAASC)grant; Coordinación General Académica e Innovación (CGAI-UdeG), PRODEP-SEP UDG-CA-499; Institute of Cosmic Ray Research (ICRR), University of Tokyo, H.F. acknowledges support by NASA under award number 80GSFC21M0002. We also acknowledge the significant contributions over many years of Stefan Westerhoff, Gaurang Yodh and Arnulfo Zepeda Dominguez, all deceased members of the HAWC collaboration. Thanks to Scott Delay, Luciano Díaz and Eduardo Murrieta for technical support.

Full Authors List: HAWC Collaboration

A.U. Abeysekara[48], A. Albert[21], R. Alfaro[14], C. Alvarez[41], J.D. Álvarez[40], J.R. Angeles Camacho[14], J.C. Arteaga-Velázquez[40], K. P. Arunbabu[17], D. Avila Rojas[14], H.A. Ayala Solares[28], R. Babu[25], V. Baghmanyan[15], A.S. Barber[48], J. Becerra Gonzalez[11], E. Belmont-Moreno[14], S.Y. BenZvi[29], D. Berley[39], C. Brisbois[39], K.S. Caballero-Mora[41], T. Capistrán[12], A. Carramiñana[18], S. Casanova[15], O. Chaparro-Amaro[3], U. Cotti[40], J. Cotzomi[8], S. Coutiño de León[18], E. De la Fuente[46], C. de León[40], L. Diaz-Cruz[8], R. Diaz Hernandez[18], J.C. Díaz-Vélez[46], B.L. Dingus[21], M. Durocher[21], M.A. DuVernois[45], R.W. Ellsworth[39], K. Engel[39], C. Espinoza[14], K.L. Fan[39], K. Fang[45], M. Fernández Alonso[28], B. Fick[25], H. Fleischhack[51,11,52], J.L. Flores[46], N.I. Fraija[12], D. Garcia[14], J.A. García-González[20], J. L. García-Luna[46], G. García-Torales[46], F. Garfias[12], G. Giacinti[22], H. Goksu[22], M.M. González[12], J.A. Goodman[39], J.P. Harding[21], S. Hernandez[14], I. Herzog[25], J. Hinton[22], B. Hona[48], D. Huang[25], F. Hueyotl-Zahuantitla[41], C.M. Hui[23], B. Humensky[39], P. Hüntemeyer[25], A. Iriarte[12], A. Jardin-Blicq[22,49,50], H. Jhee[43], V. Joshi[7], D. Kieda[48], G J. Kunde[21], S. Kunwar[22], A. Lara[17], J. Lee[43], W.H. Lee[12], D. Lennarz[9], H. León Vargas[14], J. Linnemann[24], A.L. Longinotti[12], R. López-Coto[19], G. Luis-Raya[44], J. Lundeen[24], K. Malone[21], V. Marandon[22], O. Martinez[8], I. Martinez-Castellanos[39], H. Martínez-Huerta[38], J. Martínez-Castro[3], J.A.J. Matthews[42], J. McEnery[11], P. Miranda-Romagnoli[34], J.A. Morales-Soto[40], E. Moreno[8], M. Mostafá[28], A. Nayerhoda[15], L. Nellen[13], M. Newbold[48], M.U. Nisa[24], R. Noriega-Papaqui[34], L. Olivera-Nieto[22], N. Omodei[32], A. Peisker[24], Y. Pérez Araujo[12], E.G. Pérez-Pérez[44], C.D. Rho[43], C. Rivière[39], D. Rosa-Gonzalez[18], E. Ruiz-Velasco[22], J. Ryan[26], H. Salazar[8], F. Salesa Greus[15,53], A. Sandoval[14], M. Schneider[39], H. Schoorlemmer[22], J. Serna-Franco[14], G. Sinnis[21], A.J. Smith[39], R.W. Springer[48], P. Surajbali[22], I. Taboada[9], M. Tanner[28], K. Tollefson[24], I. Torres[18], R. Torres-Escobedo[30], R. Turner[25], F. Ureña-Mena[18], L. Villaseñor[8], X. Wang[25], I.J. Watson[43], T. Weisgarber[45], F. Werner[22], E. Willox[39], J. Wood[23], G.B. Yodh[35], A. Zepeda[4], H. Zhou[30]

[1]Barnard College, New York, NY, USA, [2]Department of Chemistry and Physics, California University of Pennsylvania, California, PA, USA, [3]Centro de Investigación en Computación, Instituto Politécnico Nacional, Ciudad de México, México, [4]Physics Department, Centro de Investigación y de Estudios Avanzados del IPN, Ciudad de México, México, [5]Colorado State University, Physics Dept., Fort Collins, CO, USA, [6]DCI-UDG, Leon, Gto, México, [7]Erlangen Centre for Astroparticle Physics, Friedrich Alexander Universität, Erlangen, BY, Germany, [8]Facultad de Ciencias Físico Matemáticas, Benemérita Universidad Autónoma de Puebla, Puebla, México, [9]School of Physics and Center for Relativistic Astrophysics, Georgia Institute of Technology, Atlanta, GA, USA, [10]School of Physics Astronomy and Computational Sciences, George Mason University, Fairfax, VA, USA, [11]NASA Goddard Space Flight Center, Greenbelt, MD, USA, [12]Instituto de Astronomía, Universidad Nacional Autónoma de México, Ciudad de México, México, [13]Instituto de Ciencias Nucleares, Universidad Nacional Autónoma de México, Ciudad de México, México, [14]Instituto de Física, Universidad Nacional Autónoma de México, Ciudad de México, México, [15]Institute of Nuclear Physics, Polish Academy of Sciences, Krakow, Poland, [16]Instituto de Física de São Carlos, Universidade de São Paulo, São Carlos, SP, Brasil, [17]Instituto de Geofísica, Universidad Nacional Autónoma de México, Ciudad de México, México, [18]Instituto Nacional de Astrofísica, Óptica y Electrónica, Tonantzintla, Puebla, México, [19]INFN Padova, Padova, Italy, [20]Tecnologico de Monterrey, Escuela de Ingeniería y Ciencias, Ave. Eugenio Garza Sada 2501, Monterrey, N.L., 64849, México, [21]Physics Division, Los Alamos National Laboratory, Los Alamos, NM, USA, [22]Max-Planck Institute for Nuclear Physics, Heidelberg, Germany, [23]NASA Marshall Space Flight Center, Astrophysics Office, Huntsville, AL, USA, [24]Department of Physics and Astronomy, Michigan State University, East Lansing, MI, USA, [25]Department of Physics, Michigan Technological University, Houghton, MI, USA, [26]Space Science Center, University of New Hampshire, Durham, NH, USA, [27]The Ohio State University at Lima, Lima, OH, USA, [28]Department of Physics, Pennsylvania State University, University Park, PA, USA, [29]Department of Physics and Astronomy, University of Rochester, Rochester, NY, USA, [30]Tsung-Dao Lee Institute and School of Physics and Astronomy, Shanghai Jiao Tong University, Shanghai, China, [31]Sungkyunkwan University, Gyeonggi, Rep. of Korea, [32]Stanford University, Stanford, CA, USA, [33]Department of Physics and Astronomy, University of Alabama, Tuscaloosa, AL, USA, [34]Universidad Autónoma del Estado de Hidalgo, Pachuca, Hgo., México, [35]Department of Physics and Astronomy, University of California, Irvine, Irvine, CA, USA, [36]Santa Cruz Institute for Particle Physics, University of California, Santa Cruz, Santa Cruz, CA, USA, [37]Universidad de Costa Rica, San José , Costa Rica, [38]Department of Physics and Mathematics, Universidad de Monterrey, San Pedro Garza García, N.L., México, [39]Department of Physics, University of Maryland, College Park, MD, USA, [40]Instituto de Física y Matemáticas, Universidad Michoacana de San Nicolás de Hidalgo, Morelia, Michoacán, México, [41]FCFM-MCTP, Universidad Autónoma de Chiapas, Tuxtla Gutiérrez, Chiapas, México, [42]Department of Physics and Astronomy, University of New Mexico, Albuquerque, NM, USA, [43]University of Seoul, Seoul, Rep. of Korea, [44]Universidad Politécnica de Pachuca, Pachuca, Hgo, México, [45]Department of Physics, University of Wisconsin-Madison, Madison, WI, USA, [46]CUCEI, CUCEA, Universidad de Guadalajara, Guadalajara, Jalisco, México, [47]Universität Würzburg, Institute for Theoretical Physics and Astrophysics, Würzburg, Germany, [48]Department of Physics and Astronomy, University of Utah, Salt Lake City, UT, USA, [49]Department of Physics, Faculty of Science, Chulalongkorn University, Pathumwan, Bangkok 10330, Thailand, [50]National Astronomical Research Institute of Thailand (Public Organization), Don Kaeo, MaeRim, Chiang Mai 50180, Thailand, [51]Department of Physics, Catholic University of America, Washington, DC, USA, [52]Center for Research and Exploration in Space Science and Technology, NASA/GSFC, Greenbelt, MD, USA, [53]Instituto de Física Corpuscular, CSIC, Universitat de València, Paterna, Valencia, Spain